

A Comparative Neutronic Core Design Study of the NQ150 Lead-Cooled Fast Reactor with Plutonium-Based Nitride and Metallic Fuels

Geunyoung Choi^a, Seungnam Lee^a, Ser Gi Hong^{a*} and Ehud Greenspan^{b,c}

^aDept. of Nuclear Engineering, Hanyang University, 222 Wangsimni-ro, Seongdong-gu, Seoul, Korea

^bNuqleon Research Ltd., Israel

^cProfessor Emeritus, University of California, Berkeley, CA, USA

*Corresponding author: hongsergi@hanyang.ac.kr

***Keywords : Lead-cooled fast reactor, Nitride fuel, Metallic fuel, Enrichment zoning**

1. Introduction

Lead-cooled Fast Reactors (LFRs) are one of the Generation IV reactor concepts. They operate with a fast neutron spectrum and can be configured for either a closed fuel cycle or a once-through fuel cycle with a small burnup reactivity swing over a long life.

This study performs a preliminary core neutronics design analysis for the NQ150 reactor concept under development by Nuqleon Research Ltd. The NQ150 concept is based on the ENHS LFR design [1], which was adopted as the reference concept because its core design philosophy is well aligned with the primary objective of NQ150: long cycle operation without refueling and with a small burnup reactivity swing. The ENHS concept was originally developed as a once-for-life lead-cooled fast reactor in which the burnup reactivity swing over a long core life is controlled through adjustment of the pitch-to-diameter ratio and fissile loading. The NQ150 concept targets a thermal power of 360 MWth, approximately three times that of previously studied ENHS cores.

The objective of this work is to achieve a core cycle length of at least 10 Effective Full Power Years (EFPYs) without refueling while maintaining a limited burnup reactivity swing. In this initial phase, the analysis focuses on neutronic feasibility and on the evolution of the effective multiplication factor (k_{eff}) during burnup.

This study evaluates two fuel options. One option is PuN-deplUN nitride fuel and the other is Pu-deplU-Zr10 metallic fuel. For each fuel type, the lattice Pitch-to-Diameter ratio is varied to identify the configuration that satisfies the 10 EFPYs design target. The effect of radial enrichment zoning on power distribution is also investigated by comparing a multi-zone enrichment core with a single-enrichment core at the same Pitch-to-Diameter ratio.

This work presents preliminary core neutronics design results for the NQ150 concept and provides a basis for subsequent analyses of safety-related parameters and extended core cycle length limits.

2. Computational Code and Methodology

Core depletion analysis was performed using the Serpent 2 continuous-energy Monte Carlo code developed by VTT [2]. Continuous-energy cross sections

from the ENDF/B-VIII.0 library were employed for neutron transport and burnup calculations. A full-core three-dimensional model was adopted, with fuel pin-level heterogeneity explicitly represented.

The core was simulated at the nominal thermal power of 360 MWth. Depletion calculations were carried out up to 80 burnup steps to track the evolution of k_{eff} over the entire cycle. The k_{eff} at Beginning-of-Cycle (BOC) was set to 1.004 by adjusting the initial plutonium mass fraction. The core cycle length was defined as the burnup step at which k_{eff} decreased below 1.0025. This criterion was adopted to maintain a margin in reactivity evaluation during preliminary design assessment. The selected threshold provides a small reactivity margin to accommodate Monte Carlo statistical uncertainty, the preliminary scoping nature of the present study, and modeling simplifications adopted in this initial design phase.

All calculations were performed under identical geometric and material assumptions for both fuel types to enable direct comparison of neutronic behavior as a function of the Pitch-to-Diameter ratio.

3. Core Model and Fuel Specification

3.1. Reactor Specifications and Zoning Strategy

The NQ150 reactor analyzed in this study is based on the ENHS core design [3]. The design targets a thermal power of 360 MWth, which is approximately three times that of the reference ENHS core leading to higher power density.

Table 1. Main design parameters of NQ150.

Design Parameter	Value
Thermal power	360 MWth
Coolant material	Pb
Active core height	125 cm
Core diameter	230 cm
Fuel material	PuN-deplUN or Pu-deplU-Zr10
Fuel diameter	1.30 cm

Cladding material	HT-9
Cladding thickness	0.13 cm
Absorber	B ₄ C, 92% ¹⁰ B (75% nominal density)
Radial reflector material	Pb 100%
Radial reflector thickness	70cm

The core adopts a ductless configuration in which fuel rods are arranged in a uniform hexagonal lattice and supported by grid plates. The active core height is 125 cm and the core diameter is 230 cm. A radial reflector with a thickness of 70 cm surrounds the active core. The reflector material is lead. Lead is used as the coolant. HT-9 is used as the cladding material. Boron carbide is used as the neutron absorber. The axial reflector region inside the fuel rod is modeled as HT-9. The main design parameters are summarized in Table 1.

The metallic fuel is a Pu-^{depl}U-Zr10 alloy (10 wt% Zirconium), based on data from the Integral Fast Reactor (IFR) program. For Pu-^{depl}U-Zr10 fuel, the nominal density is 15.85 g/cm³. A smear density of 75% was assumed to accommodate swelling of fuel, resulting in an effective density of approximately 11.89 g/cm³. A smear density of 87% was assumed for the PuN-^{depl}UN nitride fuel, resulting in an effective density of approximately 12.5 g/cm³. For both fuel types, the plutonium used for this comparative analysis is derived from PWR spent nuclear fuel discharged at 50 GWd/tHM and cooled for 10 years. The plutonium isotopic composition used in this study is summarized in Table 2 and was applied identically to both fuel concepts.

In addition to the radial enrichment zoning, an axial central fuel slug with a plutonium mass fraction of 8 wt% was introduced in all fuel pins. The slug has a height of 6 cm and is located at the mid-plane of the active core. This axial modification was implemented to reduce the local power density near the structural grid region, where heat transfer to the lead coolant may be partially impeded.

Table 2. Initial Plutonium isotopic composition.

Isotope	Weight fraction
²³⁸ Pu	0.03180
²³⁹ Pu	0.56350
²⁴⁰ Pu	0.26600
²⁴¹ Pu	0.08020
²⁴² Pu	0.05830

3.2. Radial Zoning Strategy

To reduce radial power peaking, the active core was divided into six concentric radial zones. Each zone was defined to contain the same number of fuel pins. The plutonium enrichment was adjusted by zone to flatten the

radial power distribution. The radial zoning scheme is shown in Fig. 1.

The reference ENHS design employed a Pitch-to-Diameter (P/D) ratio of 1.45 for the PuN-^{depl}UN fuel and 1.36 for the Pu-^{depl}U-Zr10 metallic fuel [3]. In this study, a common baseline value of 1.36 was adopted for both fuel concepts to enable direct comparison under the modified NQ150 core configuration.

Then, the P/D ratio varied while maintaining a fixed active core diameter of 230 cm. A parametric study was conducted by gradually reducing the P/D ratio from 1.36 down to 1.20. For each P/D ratio, the total number of fuel pins loaded within the fixed core diameter was adjusted, resulting in corresponding changes in lattice pitch.

The zoning configuration was applied at the selected P/D ratio determined from the parametric analysis. A single-enrichment core was also analyzed at the same P/D ratio. To examine the impact of zoning, the k_{eff} evolution, reactivity curve, and power peaking factors were compared for the zoned and single-enrichment cores.

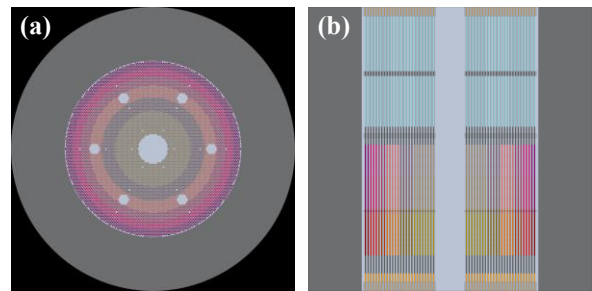


Fig. 1. NQ 150 Core Layout (a) radial view and (b) axial view.

4. Results and Discussion

4.1 P/D Ratio Sensitivity and Design Selection

A parametric analysis was conducted by reducing the P/D ratio from 1.36 to 1.20 in decrements of 0.04.

Table 3. PuN-^{depl}UN P/D Ratio Sensitivity Results.

P/D ratio	Average Pu wt%	Cycle length [EFPYs]
1.36	13.87	13.881
1.32	13.58	≥ 10
1.28	13.29	≥ 10
1.24	12.97	≥ 10
1.20	12.64	≥ 10

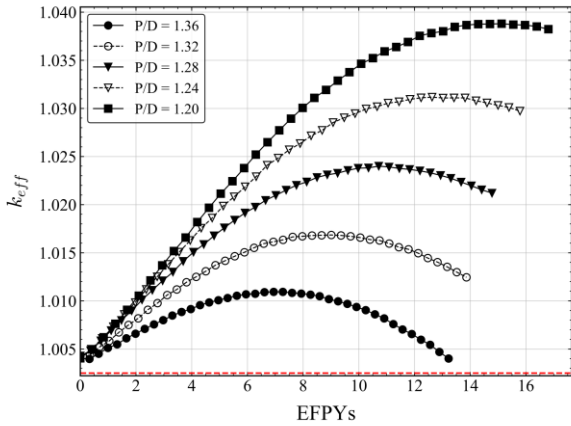


Fig. 2. Eigenvalue evolutions for the PuN-deplUN core.

For each configuration, depletion calculations were performed up to 80 burnup steps. For the PuN-deplUN case at P/D = 1.36, additional depletion steps up to 100 burnup steps were carried out to confirm the cycle length.

The sensitivity results indicate that the PuN-deplUN fuel achieves a cycle length of 13.881 EFPYs at P/D = 1.36. For the Pu-deplU-Zr10 metallic fuel, a cycle length of 11.637 EFPYs is obtained at P/D = 1.32. The corresponding plutonium mass fractions and cycle lengths are summarized in Tables 3 and 4 for the nitride and metallic fuels, respectively.

The evolution of the k_{eff} as a function of burnup is shown in Fig. 2 for the PuN-deplUN fuel and in Fig. 3 for the Pu-deplU-Zr10 fuel. A horizontal dashed line at $k_{eff} = 1.0025$ indicates the adopted cycle length criterion. Based on the results, the PuN-deplUN-fueled core at P/D = 1.36 is hereafter referred to as Design I, and the Pu-deplU-Zr10-fueled core at P/D = 1.32 is referred to as Design II.

Table 4. Pu-deplU-Zr10 P/D Ratio Sensitivity Results

P/D ratio	Average Pu wt%	Cycle length [EFPYs]
1.36	13.46	5.862
1.32	13.08	11.637
1.28	12.79	≥ 10
1.24	12.41	≥ 10
1.20	12.09	≥ 10

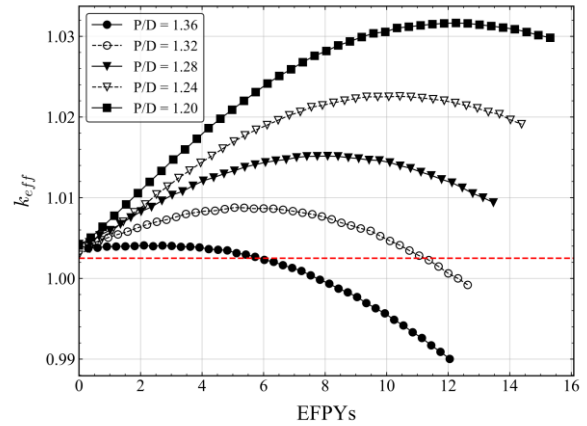


Fig. 3. Eigenvalue evolutions for the Pu-deplU-Zr10 core.

The burnup reactivity behavior of these cores is presented in Fig. 4. The effective delayed neutron fraction (β_{eff}) at BOC is 375 pcm for Design I and 379 pcm for Design II. The maximum excess reactivity is 683.75 pcm for Design I and 395.24 pcm for Design II, corresponding to approximately 1.82 \$ and 1.04 \$, respectively. These results indicate that Design I exhibits a larger excess reactivity relative to its delayed neutron fraction, implying a higher reactivity control demand under identical operating conditions.

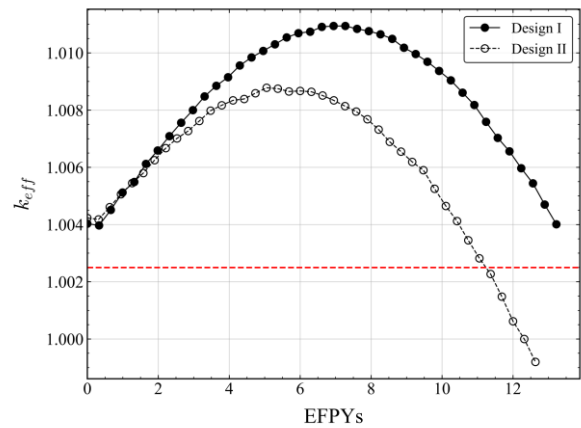


Fig. 4. Reactivity evolutions for Design I and II.

4.2 Power Distribution of the Selected Designs

The evolution of the radial power peaking factor (F_r) and the total power peaking factor (F_q) for Design I and Design II are shown in Fig. 5 and Fig. 6, respectively. For both designs, the peaking factors increase gradually with burnup. At BOC, F_r is 1.07 for Design I and 1.09 for Design II, increasing to 1.32 for both designs toward End-of-Cycle (EOC). The F_q increases from 1.46 to 1.75 for Design I and from 1.54 to 1.75 for Design II over the same period.

The overall magnitude and trend of F_r and F_q are comparable between Design I and Design II. Under the

selected P/D conditions, the difference in fuel type does not significantly affect the power distribution behavior.

Although the selected P/D configurations satisfy the preliminary cycle length requirement, the power peaking factors gradually increase toward EOC conditions. This trend suggests that further optimization of the enrichment distribution may be required to mitigate the late-cycle power peaking behavior although they are in acceptable level comparing with commercial PWRs.

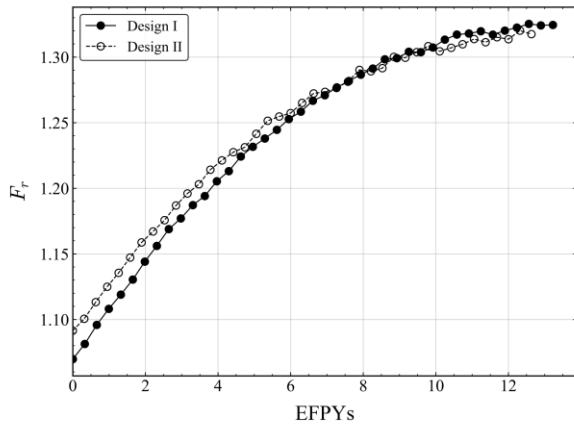


Fig. 5. Evolution of radial power peaking factor (F_r) for Design I and Design II.

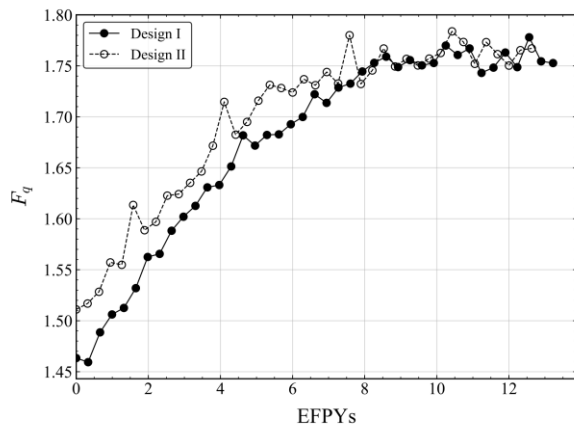


Fig. 6. Evolution of 3D power peaking factor (F_q) for Design I and Design II.

The peak linear heat rate (PLHR) for the selected designs is summarized as follows. For Design I, the PLHR increases from 401.93 W/cm at BOC to 490.00 W/cm at EOC. For Design II, the corresponding values are 389.63 W/cm at BOC and 468.96 W/cm at EOC.

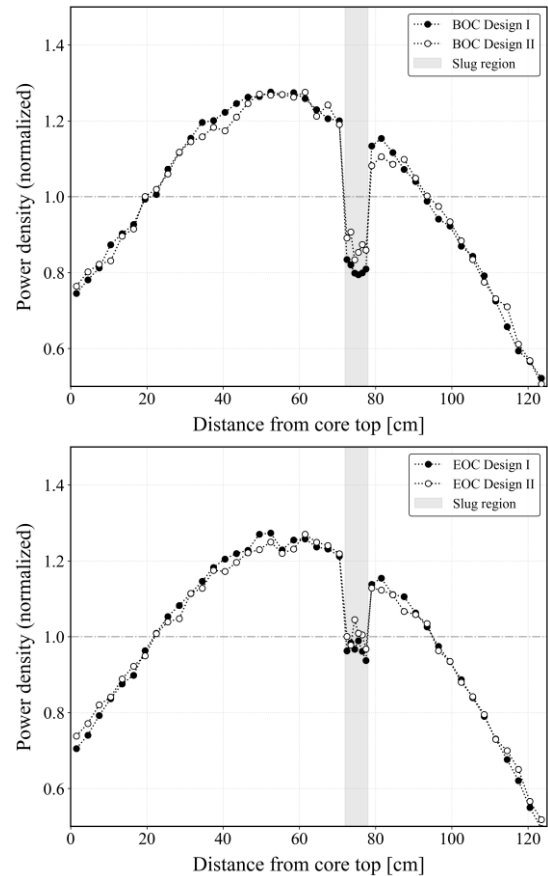


Fig. 7. Axial power distribution in the hottest channel at (a) BOC and (b) EOC.

The axial power distributions at BOC and EOC are shown in Fig. 7. A local power depression is observed in the axial slug region, where the low-enrichment zone is located. However, the axial power distribution remains close to a cosine shape, and the central low-enrichment slug provides only limited mitigation of the overall power peaking. These results indicate that the present axial slug design achieves only marginal improvement in axial power flattening. In future work, a more comprehensive axial enrichment zoning strategy along the entire active height needs to be considered to obtain a more uniform axial power distribution.

4.3 Zoning Effect Analysis

The impact of radial enrichment zoning on neutronic performance and power distribution was evaluated for both designs.

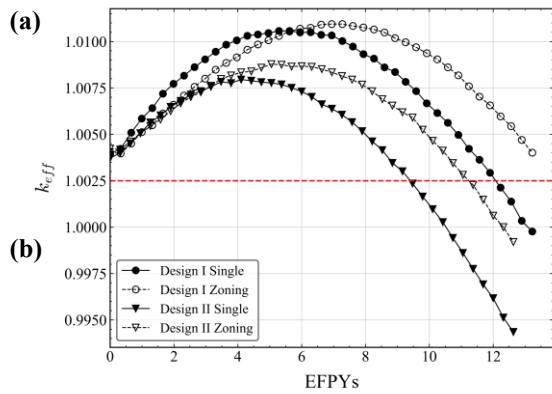


Fig. 8. Evolution of k_{eff} for Single and Zoned Cores.

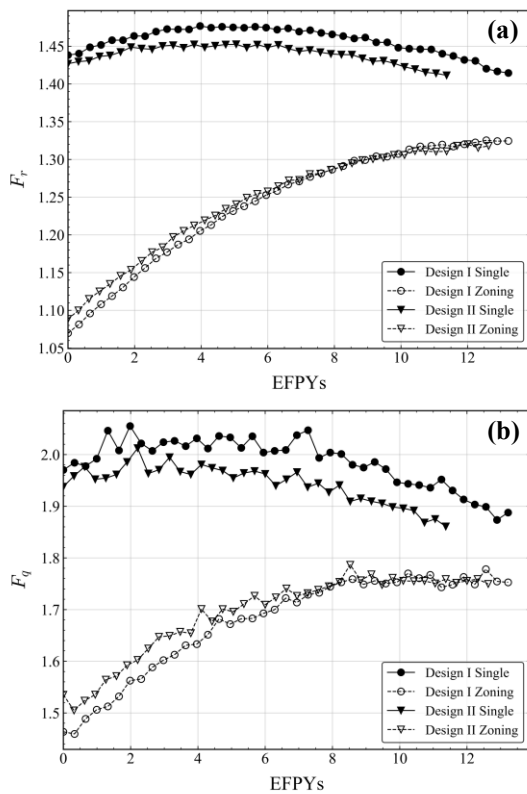


Fig. 9. Evolution of power peaking factors for single and zoned configurations: (a) F_r and (b) F_q .

For Design I, the cycle length increases from 12.079 EFPYs in the single-enrichment configuration to 13.881 EFPYs with zoning, while for Design II it increases from 9.800 EFPYs to 11.637 EFPYs. In both cases, radial zoning extends the core cycle length by approximately 1.8 EFPYs and maintains higher reactivity throughout the cycle, as shown in Fig. 8.

Zoning also reduces both the F_r and the F_q over burnup, resulting in a flatter radial power distribution compared to the single-enrichment configuration. The corresponding evolutions of the peaking factors and the radial power distributions are shown in Fig. 9 and Fig. 10, respectively.

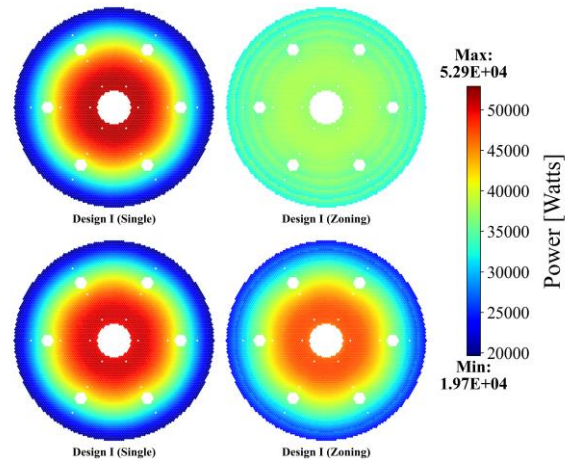


Fig. 10. Radial power maps of Design I comparing single and zoned configurations at (a) BOC and (b) EOC.

4.4 Fuel Comparison

At BOC, β_{eff} is 375 pcm for Design I and 379 pcm for Design II, indicating little sensitivity to fuel type under the same plutonium composition. However, the maximum excess reactivity differs noticeably, with Design I exhibiting 1.82 \$ and Design II showing 1.04 \$. Although β_{eff} is similar, Design I accumulates a larger excess reactivity over burnup, implying a higher reactivity control requirement.

Design I also achieves a longer cycle length at its optimal P/D ratio. Previous studies [3] indicate that nitride fuels generally possess higher heavy metal density and more favorable neutron balance characteristics than metallic fuels, which is consistent with the longer cycle length and larger reactivity accumulation observed for Design I.

In terms of power distribution, the evolution of F_r and F_q is similar for both designs, and the differences in peaking factors remain small throughout the cycle. Under the selected lattice and zoning configuration, fuel type does not dominate power peaking behavior.

Overall, Design I provides longer cycle performance with larger excess reactivity, whereas Design II offers reduced excess reactivity with a relatively shorter cycle length.

5. Conclusion

In conclusion, preliminary neutronic analyses demonstrated that the NQ150 LFR cores fueled with $\text{PuN}_{-depl}\text{UN}$ and $\text{Pu}_{-depl}\text{U-Zr10}$ can achieve operation over 10 EFPYs while maintaining a limited burnup reactivity swing. The nitride-fueled core attains the target cycle length at a relatively larger P/D ratio compared to the metallic-fueled core. However, its larger excess reactivity implies a higher requirement for reactivity control and shutdown margin.

The Pu-^{depl}U–Zr10 metallic-fueled core exhibits slightly lower radial and three-dimensional power peaking factors, indicating a more moderate power distribution behavior.

Future work will determine the maximum allowable core lifetime under the 200 dpa radiation damage constraint of HT9 cladding and evaluate reactivity coefficients and additional safety parameters to further assess the inherent safety characteristics of the proposed designs.

ACKNOWLEDGMENTS

This work was supported by the Korea Institute of Energy Technology Evaluation and Planning (KETEP) and the Ministry of Climate, Energy & Environment (MCEE) of the Republic of Korea (No. RS-2024-00398867).

REFERENCES

- [1] E. Greenspan *et al.*, “Innovations in the ENHS reactor design and fuel cycle,” *Prog. Nucl. Energy*, vol. 50, no. 2–6, pp. 129–139, Mar. 2008, doi: 10.1016/j.pnucene.2007.10.022.
- [2] J. Leppänen, M. Pusa, T. Viitanen, V. Valtavirta, and T. Kaltiaisenaho, “The Serpent Monte Carlo code: Status, development and applications in 2013,” *Ann. Nucl. Energy*, vol. 82, pp. 142–150, Aug. 2015, doi: 10.1016/j.anucene.2014.08.024.
- [3] S. G. Hong, E. Greenspan, and Y. I. Kim, “The Encapsulated Nuclear Heat Source (ENHS) Reactor Core Design,” *Nucl. Technol.*, vol. 149, no. 1, pp. 22–48, Jan. 2005, doi: 10.13182/NT05-A3577.